A Procedure for Damage-Based Seismic Design of Moment Frame Structures

Farhad Behnamfar (farhad@iut.ac.ir)
Isfahan University of Technology https://orcid.org/0000-0002-4435-3540
Ali Hosseini-Rad
Isfahan University of Technology
Yusef Mesr Habiby
Isfahan University of Technology

Research Article

Keywords: seismic design, damage based, moment frame, Park-Ang, drift.

Posted Date: July 20th, 2021

DOI: https://doi.org/10.21203/rs.3.rs-721002/v1

A procedure for damage-based seismic design of moment frame structures

Farhad Behnamfar, Ali Hosseini-Rad, Yusef Mesr Habiby

Department of Civil Engineering, Isfahan University of Technology, Isfahan 8415683111, Iran

Corresponding author, Email: farhad@iut.ac.ir

Abstract

A new method for seismic design of structures with the aim of controlling earthquake damage to a prescribed level is presented in this paper. The main idea is determining a design story drift in correlation to a selected damage index value. For this purpose, the Park-Ang damage index is correlated with a damage index that simply uses only the maximum story drift. Through performing several nonlinear dynamic analyses of selected moment frame steel structures and regression analysis, it is shown that such a correlation is possible by a simple linear relation. Beginning from a desired value of the damage index, the design story drift is calculated using the developed linear equation and the same buildings are designed using a displacement-base procedure. Results of the nonlinear dynamic analysis of the buildings show that the maximum story damage index under a suit of spectrum compatible ground motions is consistent with the selected initial damage index using the proposed procedure.

Keywords: seismic design, damage based, moment frame, Park-Ang, drift.

1. Introduction

The idea goal of a seismic design procedure is limiting the seismic damage of a building system under the design earthquake motion to a repairable level. In the last 100 years, this goal has been pursued by determining an appropriate lateral strength, based on seismicity and building system, and then containing the maximum story drift. This design approach is known as the force-based procedure of seismic design. It makes the basis of the current earthquake resistant design codes of practice. The existing buildings represent the outcome of such a practice and they have shown an improving trend of seismic behavior during years as the design codes gradually evolved. In more recent years, there has been a tendency to give the displacement-checking part of the procedure more importance by exchanging it with the strength-design part in the sequence of seismic design. In other words, it was desired to determine the required lateral strength based on the selected maximum lateral displacement of the stories. It is now called the displacement-based procedure of seismic design. It has grown to a displacement-based seismic design code called DBD09 and then DBD12 in 2012 [1]. The newer idea, followed in this research, is to make the mentioned procedure more sensible by enabling it to be started from a certain selected seismic damage level such that the user can decide on the expected intensity of earthquake damage based on the function, value, and anticipated final age of the building among other factors. Quantifying seismic damage has been made possible much sooner than emerge of the damage-based design idea by developing the damage index. A damage index represents the intensity of damage in a structural member, at a story, or overall in a building. It is based on maximum lateral deformations, cyclically-stored plastic energy, or a combination of both. There has been several damage indices proposed by different researchers, such as those of Powell and Allahabadi based on maximum deformation [2], and the combined indices proposed

by Krawinkler and Zohrei [3], Bozorgnia and Bertero [4], and Park and Ang [5]. The later damage index, modified by Kunnath et al. [6], has gained more acceptance because of it is versatility and consistency with the results of experiments. As it is the basic tool in the current research, it will be explained in more detail in the next sections.

Developing practical procedures for seismic damage-based design has been tried by a number of researchers in recent years. Panyakapo [7] essentially presented graphs of the damage index as a function of demand spectral displacements and accelerations. The developed diagrams were called the demand-capacity curves based on seismic damage. They used the pushover analysis for determining the lateral capacity and the Park-Ang damage index for the mentioned curves as the main output of their study. Jiang et al. [8] proposed a damage control procedure by presenting a seismic design path in which the maximum drift of an equivalent single-degree-of-freedom (SDOF) system was checked first using the results of analysis of the main building. Kamaris et al. [9] developed a damage-based seismic design procedure for moment frame steel structures including effects of stiffness and strength degradation in higher cycles of deformation. For the basis of their procedure, they used a damage index developed by the same researchers [10]. Although their method was shown to be successful in predicting the maximum damage under spectrum-compatible ground motions, necessity for use of time consuming nonlinear dynamic analysis put the procedure practically out of hand. Ke and Michael [11] expressed the performance design method on the basis of damage control in moment frames combined with energy dissipation bay frames (EDBs). The results exhibited that all prototypes of steel moment frames combined with EDBs were capable to reach the damage control behavior based upon the considered drift value.

It has been shown that a good match exists between what is predicted by some of the damage indices and the story drift [12]. The correlation relations were presented as conversion curves between the damage index and the maximum story drift. Such a relation makes it possible to devise a practical procedure for damage-based design. Behnamfar and Kazemi [13] showed that developing a linear relation for conversion of the Park-Ang damage index to the maximum story drift is possible at least for moment frames, simply based on the number of stories. This is the main idea of the present study. In this paper, a conversion equation is presented for a range of moment frame buildings by which it is possible to calculate the design drift based on the desired value of the Park-Ang damage index. Regression analysis of the results of several nonlinear dynamic analysis is used for the same purpose. Then the suggested damage-based design procedure is presented within the context of the displacement-design approach. Finally, it is shown that the designed buildings follow the maximum damage index laid down for their design.

2. Developing the damage-drift relation

2.1. General

In this section it is aimed at developing an equation relating the maximum story drift to the maximum damage index of the story. The Park-Ang damage index as modified by Kunnath et al. [6], is selected as the basis of calculations. It is an index combined of the effects of maximum drift ratio and the cumulative stored plastic energy. It is shown as follows:

$$DI = \frac{\theta_m - \theta_y}{\theta_u - \theta_y} + \beta \frac{\int dE}{M_y \theta_u} \tag{1}$$

in which θ_m is the maximum rotation of the section, θ_u is the rotational capacity, θ_y is the yield rotation, M_y is the yield moment, $\int dE$ is the absorbed hysteretic energy, and β is a calibration factor representing the effect of the dissipated energy on the limit damage. β is equal to 0.4 for steel structures. Then the story damage index DI_{Story} is calculated as the weighted average of the member damage indices using Eq. (2):

$$DI_{Story} = \sum (\lambda_i)_{component} (DI_i)_{component}$$
$$(\lambda_i)_{component} = \left(\frac{E_i}{\sum E_i} \right) \quad (2)$$

in which λ_i is an energy weight factor and E_i is the absorbed energy by the *i*-th member or story.

To prepare the necessary data for developing the conversion equation, use is made of several nonlinear dynamic analyses of selected buildings and regression analysis. The mentioned buildings are introduced in the following.

2.2. The studied buildings

For developing the damage-based methodology, three buildings composed of special steel moment frames are selected. Number of stories is 4, 8, and 12. Their common plan consists of three bays each way with each bay spanning at 5 m. The story height is 3.2 m. The steel material is A36 (American standard) or St-37 (European standard) having a yield stress of 240 MPa. Box and IPE sections are used for the columns and beams, respectively. Design of the buildings is performed based on requirements of ASCE 7-16 [14] and AISC-LRFD 360-10 [15]. The dead load is calculated to be 5.7 KN/m^2 for the story floors and 6.4 KN/m^2 for the highest roof. The equivalent partition load is 1 KN/m^2. Weight of the perimeter walls is imposed as a uniform linear load. The live load is 2 KN/m^2 for the stories and 1.5 KN/m^2 for the roof.

Design seismic load is calculated based on the design spectrum. It is assumed that the buildings are located in a highly seismic area (such as Los Angeles, USA) on a firm soil (Type D, according to ASCE 7-16 [14]). With these assumptions, the design spectrum appears to be as shown in Fig. 1.

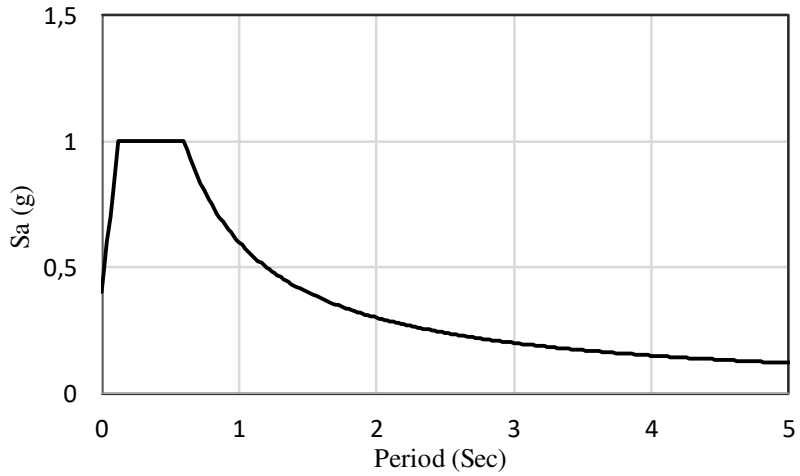

Fig. 1. The design spectrum

As a result, the beam sections emerge to be IPE240 to IPE330 for the 4-story building, IPE240 to IPE360 for the 8-story building, and IPE270 to IPE400 for the 12-story building. For the same order of buildings, the column box sections are 160×20 to 300×20 mm, 180×20 to 340×20 mm, and 180×20 to 440×30 mm. The fundamental periods of the buildings are 1.07, 1.90, and 2.19 sec for the 4, 8, and 12-story buildings, respectively.

2.3. Nonlinear modelling

The OpenSEES software [16] is selected for the response analysis of this study. There are several options for nonlinear modelling of the one-dimensional (1D) members, i.e. beams and columns, in this software. In general, modelling of the nonlinear action can be performed with good accuracy assuming that it is concentrated at the ends of the 1D members as observed more or less in reality. In the concentrated plasticity modelling approach, use can be made of nonlinear rotational (M-θ) springs, or of nonlinear fibers. Use of the latter one means dividing the section into several longitudinal fibers, each one located at the centroid of the corresponding small part of the section. Each fiber is represented by it is bilinear stress-strain relation that, in contrast with the M- θ spring, bears no degradation in stiffness and strength along its positive-slope second branch. On the other hand, again in contrast to the M-θ spring, with fiber modelling interaction of two-way flexure and axial force can be included in nonlinear analysis.

In all, it seems that use of nonlinear M-θ springs is appropriate enough if large deformations are not expected. As shown in the pushover curve of the 4-story structure in Fig. 2, the nonlinear behavior in fiber modeling and concentrated plasticity method both in the elastic and plastic regions is well matched up to the drift of 4%. Since in special moment frames columns are designed to be stronger than beams, it is not anticipated for columns of the studied buildings to develop large plastic actions. Then it is decided to use the concentrated plasticity approach throughout.

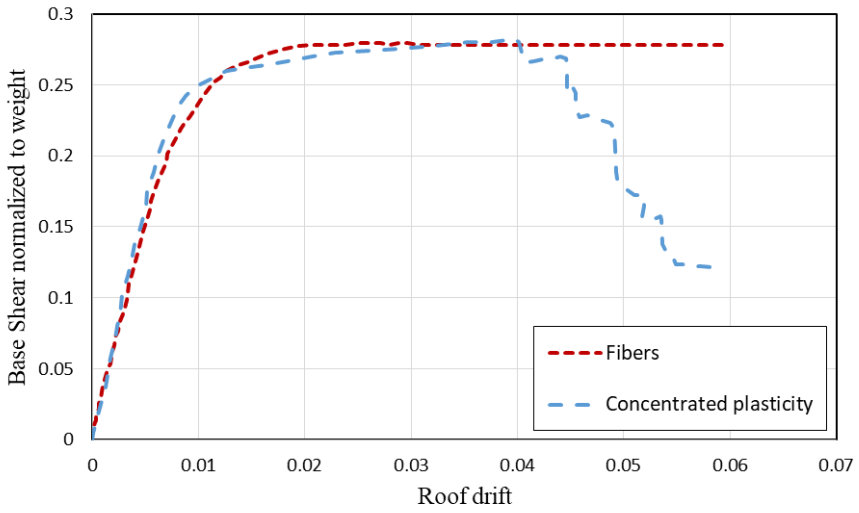

Fig. 2. Pushover curves using fiber model and the concentrated plasticity for the 4-story structure.

The M-θ path of the nonlinear springs under positive and negative moments is shown in Fig. 3.

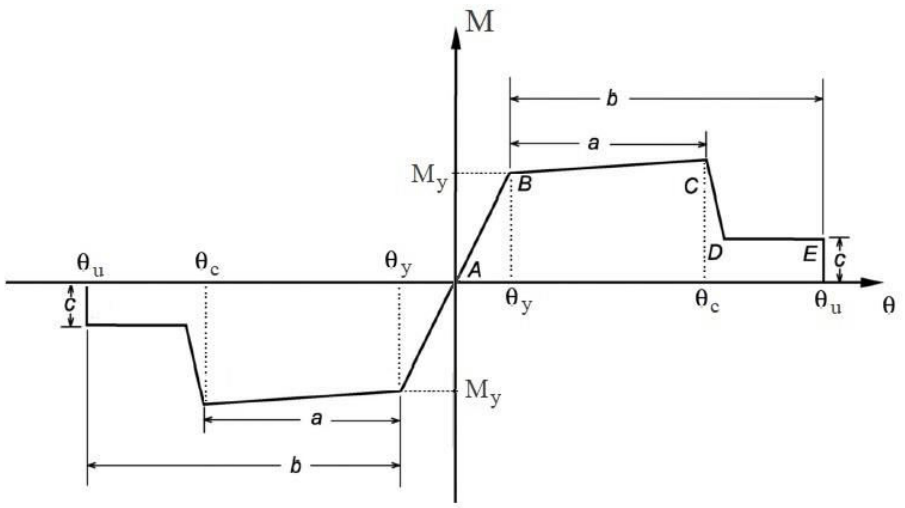

Fig. 3. The M-θ path of the nonlinear springs.

Characteristics of the M-θ curve are taken from ASCE 41-17 [17]. Besides, The cyclical deterioration rate follows the rule developed by Rahnama and Krawinkler [18]. According to this rule, the rate of strength and stiffness cyclic deterioration depends on the hysteretic energy of the component dissipated in excursions. It is considered that each component has a reference energy hysteretic dissipation capacity E_t, which is an inherent property of the components and it is independent of applied loading history. The reference hysteretic energy dissipation capacity consists of multiplying the reference cumulative rotation capacity, Λ, and the effective yield strength, M_y. Values of Λ are calculated according to the relationships developed by Lignos and Krawinkler [19], as follows, respectively for beam and column sections:

$$\Lambda = \frac{E_t}{M_y} = 495 \cdot \left(\frac{h}{t_w}\right)^{-1.34} \cdot \left(\frac{b_f}{2t_f}\right)^{-0.595} \cdot \left(\frac{c_{unit}^2 \cdot F_y}{355}\right)^{-0.360} \tag{3}$$

$$\Lambda = \frac{E_t}{M_y} = 3012 \cdot \left(\frac{D}{t}\right)^{-2.49} \cdot \left(1 - \frac{N}{N_y}\right)^{3.51} \cdot \left(\frac{c \cdot F_y}{380}\right)^{-0.20} \tag{4}$$

in which, h and t_w are the web depth and thickness, respectively, b_f and t_f are respectively width and thickness of the flange, D and t are the side dimension and thickness of the box section, N and N_y are the existing and yield axial force, F_y is the yield strength, and c is a conversion factor that equals unity when using MPa and mm dimensions.

For the M-θ springs of beams and columns, the expected bending capacity is the fully plastic moment including strain hardening effect, M_{pe}, and the yield rotation, θ_y, is calculated using the following equations:

$$\theta_y = \frac{M_{pe} L (1+\eta)}{6EI} \tag{5}$$

$$\eta = \frac{12EI}{L^2 G A_s} \tag{6}$$

in which L is the free member length, E is the modulus of elasticity, I is the moment of inertia about the axis of rotation, and G and A_s are the shear modulus and shear area, respectively. The other parameters needed for defining the M-θ curve are a, b, and c (see Fig. 3.). They represent the ductility and residual strength that are functions of compactness of the section and condition of its lateral bracing. They are taken from ASCE 41-17 [17] as listed in Table 1, along with values of θ_y .

Table 1. Values of the nonlinear modeling parameters of the M-θ springs of (a) beams, and for instance, (b) column C1 of the 4-story structure (see Fig. 3.)

(a)

Beam section	Modeling parameters					
	a	b	c	θ_y	θ_u	Λ
IPE180	0.094	0.115	0.600	0.010	0.125	2.052
IPE240	0.068	0.083	0.600	0.007	0.091	1.631
IPE300	0.055	0.067	0.600	0.006	0.074	1.319
IPE330	0.050	0.061	0.600	0.005	0.066	1.252
IPE360	0.046	0.056	0.600	0.005	0.061	1.244
IPE400	0.041	0.050	0.600	0.005	0.055	1.188
IPE450	0.037	0.045	0.600	0.004	0.050	1.155
IPE500	0.033	0.041	0.600	0.003	0.044	1.144
IPE550	0.030	0.037	0.600	0.003	0.040	1.141

(b)

Story	1	2	3	4
Column	BOX220×20			BOX140×20
N/N_y	0.125	0.0943	0.067	0.044
a	0.045	0.046	0.046	0.0789
b	0.055	0.056	0.057	0.097
c	0.6	0.6	0.6	0.6
θ_y	0.005	0.0051	0.0052	0.0088
θ_u	0.061	0.061	0.0624	0.106
Λ	6.24	6.80	7.41	23.94

Other than the beams and columns, the panel zone, encompassing part of the steel columns located at their junctions with beams are under large shear forces subjected to lateral earthquake motions. Therefore, the resulting shear deformations should be appropriately included. Since the studied buildings are composed of special moment frames, it is assumed that the panel zones are perfect regarding use of continuity plates and adequate shear strength of the column webs. Panel zone flexibility leads to intensification of the deformations and demands in the elements. For this purpose, elastic elements at the ends of beams through the column depth are used to model the panel zone deformations as shown in Fig. 4.

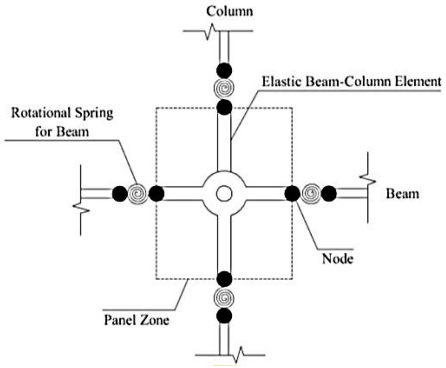

Fig. 4. Modeling of the panel zone

Characteristics of the panel zone elements are according to a 3D joint in which seven nodes (six nodes at the center of the panel zone faces and one node in the center of the panel zone), and six elastic elements are used. To these elastic elements, a section including the continuity plates and the column web is assigned. Also, the distance between face of column and plastic hinge is assumed to be zero to model the direct connection of the beam to the column. Finally, damping is presumed to be of the Rayleigh type in this study, using a damping ratio of 5%.

Adequacy of the nonlinear modelling of this study is verified by repeating the dynamic analysis of the 4-story building of Farahani et al. [20], being very similar to the 4-story building of this study, under the Loma Prieta earthquake. Results of analysis are compared in Fig. 5 for time history of the roof displacement. A very good match is observed between the outputs of the two analyses.

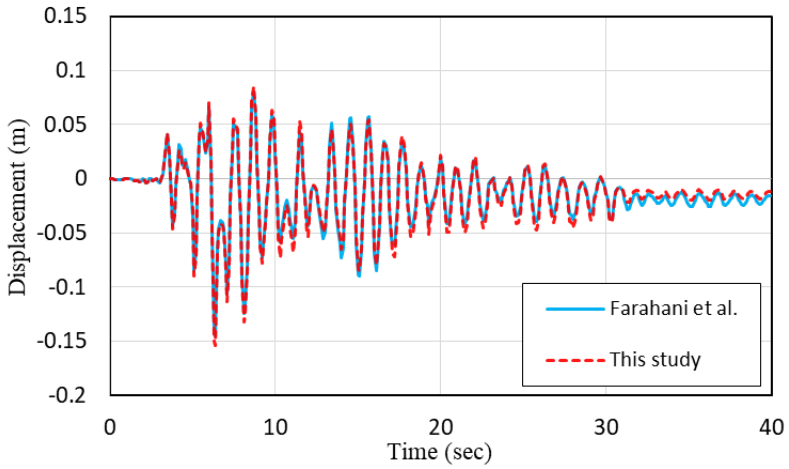

Fig. 5. Verification study: Comparing the roof time history of the 4-story building under Loma Prieta earthquake.

2.4. The selected ground motions

According to ASCE 7-16 [14], at least 11 pairs of ground motions should be selected for nonlinear dynamic analysis of each building. These earthquake motions are extracted from PEER NGA [21]. They are selected to be consistent with the characteristics of the site for which the buildings were designed, i.e. motions recorded on the soil type D in a highly seismic area in which the design magnitude M is between 6.5 and 7.5 for an epicentral distance of 20-50 km. Although, for this limited number of constraints, a too large number of earthquakes is reported within the search engine. To reduce the number to an affordable

value, 11 earthquakes with their scale factors being closer to unity are retrieved. This is a two-stage procedure. The scale factor is defined as a number that is multiplied by the resultant acceleration spectrum and modifies it such that nowhere between 0.2T and 2T periods, it falls below 90% of the design spectrum (Fig. 1.), where T is the fundamental period of the building. This is a two-stage procedure. First, a single pair of ground motions is selected by this method for every earthquake recorded at several stations. Then the scale factor calculated for the selected station is compared with the scale factors determined similarly for other earthquakes. The selected 11 sets of earthquake ground motions will possess scale factors having least distance from unity. As mentioned, the scale factors are calculated for the resultant spectrum of each earthquake. It is the square root of sum of the squares (SRSS) of the spectra of the two horizontal components of the ground motion at each period of interest.

The scale factor for selection is calculated for each earthquake as explained above. However, after the 11-pair set are selected, a unique scale factor is determined for the set by repeating the above procedure this time for the average spectrum of the 11 SRSS spectra. This way, the scale factors appear to be 1.27, 1.25, and 1.24 for the ground motions belonging to the 4, 8, and 12-story buildings, respectively.

The selected earthquake ground motions and their average SRSS spectra before and after scaling are shown in Table 2 and Fig. 6, respectively.

Table 2. The ground motions selected for (a) 4-story (b) 8-story (c) 12-story buildings.

Order	NGA no.	Earthquake name	Magnitude	Year	Dist. (km)	Shear wave velocity (m/sec)
(a)						
1	20	Northern Calif-03	6.5	1954	26.72	219.31
2	68	San Fernando	6.61	1972	22.77	316.46
3	169	Imperial Valley-06	6.53	1979	22.03	242.05
4	778	Loma Prieta	6.93	1989	24.52	215.54
5	826	Cape Mendocino	7.01	1992	40.23	337.46
6	900	Landers	7.28	1992	23.62	353.63
7	987	Northridge-01	6.69	1994	20.36	321.91
8	1107	Kobe_ Japan	6.9	1995	22.5	312
9	4853	Chuetsu-oki_ Japan	6.8	2007	25.68	294.71
10	5814	Iwate_ Japan	6.9	2008	31.07	248.19
11	6923	Darfield_ New Zealand	7.0	2010	30.5	255.0
(b)						
1	20	Northern Calif-03	6.5	1954	26.72	219.31
2	68	San Fernando	6.61	1972	22.77	316.46
3	169	Imperial Valley-06	6.53	1979	22.03	242.05
4	778	Loma Prieta	6.93	1989	24.52	215.54
5	900	Landers	7.28	1992	23.62	353.63
6	987	Northridge-01	6.69	1994	20.36	321.91
7	1110	Kobe_Japan	6.9	1995	24.78	256
8	4849	Chuetsu-Oki_Japan	6.8	2007	20.71	342.74
9	5814	Iwate_ Japan	6.9	2008	31.07	248.19
10	5988	El Mayor-Cucapah_ Mexico	7.2	2010	30.18	196
11	6923	Darfield_ New Zealand	7.0	2010	30.5	255.0
(c)						
1	20	Northern Calif-03	6.5	1954	26.72	219.31
2	68	San Fernando	6.61	1972	22.77	316.46
3	169	Imperial Valley-06	6.53	1979	22.03	242.05
4	777	Loma Prieta	6.93	1989	27.33	198.77

5	900	Landers	7.28	1992	23.62	353.63
6	987	Northridge-01	6.69	1994	20.36	321.91
7	1110	Kobe_Japan	6.9	1995	24.78	256
8	4849	Chuetsu-Oki_Japan	6.8	2007	20.71	342.74
9	5814	Iwate_ Japan	6.9	2008	31.07	248.19
10	5988	El Mayor-Cucapah_ Mexico	7.2	2010	30.18	196
11	6923	Darfield_ New Zealand	7.0	2010	30.5	255.0

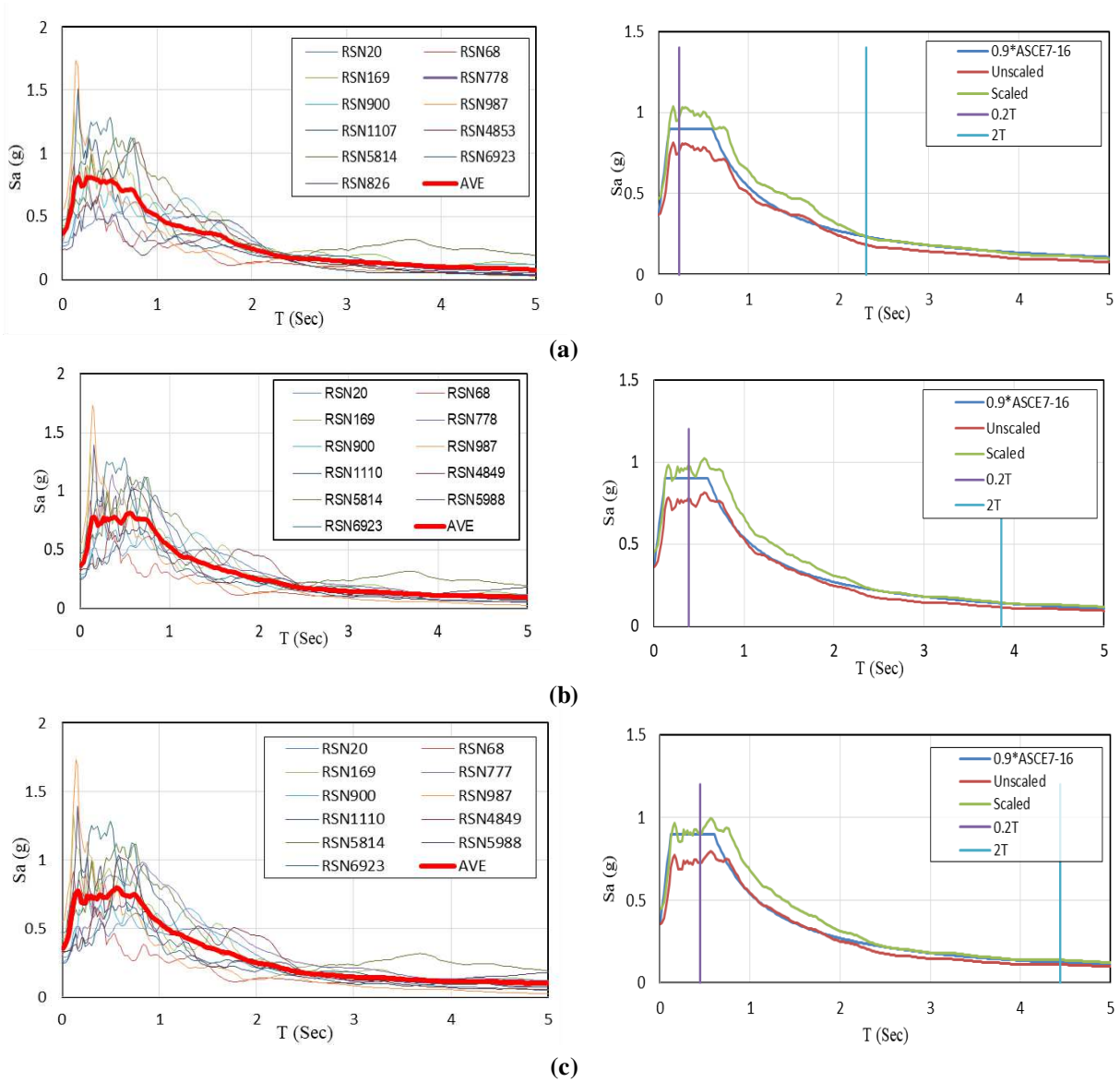

Fig. 6. Acceleration spectra of the selected records for (a) 4-story (b) 8-story (c) 12-story buildings.

2.5. Nonlinear dynamic analysis results

The structures introduced in Sec. 2.2 are analyzed under the ground motions of Sec. 2.4. As a result, time history of the damage index is calculated at each story using Eq. (2) and its maximum value is determined

for each story in each earthquake. Similarly, maximum story drifts are determined. Table 3 shows the maximum story drift ratios.

Table 3. Maximum drift ratios of each story under each earthquake. (a) 4-story, (b) 8-story, (c) 12-story buildings.

(a)

NGA no.	Story 1	Story 2	Story 3	Story 4
	Max drift ratio			
20	0.015	0.018	0.017	0.015
68	0.007	0.009	0.010	0.011
169	0.017	0.018	0.014	0.013
778	0.012	0.014	0.014	0.015
826	0.009	0.013	0.013	0.010
900	0.011	0.014	0.013	0.013
987	0.013	0.017	0.015	0.011
1107	0.011	0.015	0.015	0.014
4853	0.012	0.014	0.012	0.013
5814	0.022	0.027	0.027	0.024
6923	0.010	0.014	0.014	0.018

(b)

NGA no.	Story 1	Story 2	Story 3	Story 4	Story 5	Story 6	Story 7	Story 8
	Max drift ratio							
20	0.0099	0.0165	0.0214	0.0238	0.0233	0.0189	0.0124	0.0119
68	0.0033	0.0060	0.0068	0.0064	0.0063	0.0068	0.0067	0.0076
169	0.0083	0.0136	0.0162	0.0156	0.0157	0.0144	0.0160	0.0156
778	0.0136	0.0181	0.0188	0.0178	0.0197	0.0197	0.0159	0.0134
900	0.0047	0.0098	0.0113	0.0148	0.0205	0.0228	0.0187	0.0166
987	0.0037	0.0070	0.0096	0.0110	0.0112	0.0125	0.0119	0.0113
1110	0.0056	0.0103	0.0124	0.0128	0.0121	0.0126	0.0116	0.0138
4849	0.0096	0.0156	0.0195	0.0216	0.0212	0.0238	0.0198	0.0147
5814	0.0087	0.0141	0.0161	0.0163	0.0157	0.0201	0.0228	0.0235
5988	0.0055	0.0113	0.0150	0.0186	0.0224	0.0228	0.0176	0.0145
6923	0.0106	0.0159	0.0183	0.0182	0.0158	0.0141	0.0177	0.0191

(c)

NGA no.	Story1	Story 2	Story 3	Story 4	Story 5	Story 6	Story 7	Story 8	Story 9	Story 10	Story 11	Story 12
	Max drift ratio											
20	0.0036	0.0081	0.0107	0.0134	0.0152	0.0164	0.0166	0.0164	0.0138	0.0117	0.0101	0.0091
68	0.0027	0.0054	0.0061	0.0061	0.0059	0.0061	0.0060	0.0061	0.0060	0.0063	0.0065	0.0071
169	0.0038	0.0081	0.0097	0.0098	0.0103	0.0115	0.0129	0.0147	0.0140	0.0105	0.0128	0.0118

777	0.0106	0.0146	0.0152	0.0151	0.0165	0.0189	0.0196	0.0181	0.0165	0.0179	0.0158	0.0136
900	0.0034	0.0075	0.0094	0.0103	0.0106	0.0116	0.0137	0.0165	0.0166	0.0135	0.0117	0.0112
987	0.0027	0.0052	0.0057	0.0056	0.0055	0.0061	0.0072	0.0093	0.0108	0.0114	0.0108	0.0099
1110	0.0035	0.0081	0.0104	0.0112	0.0106	0.0093	0.0085	0.0088	0.0123	0.0148	0.0147	0.0132
4849	0.0043	0.0096	0.0127	0.0145	0.0156	0.0167	0.0171	0.0173	0.0195	0.0181	0.0141	0.0108
5814	0.0058	0.0112	0.0137	0.0144	0.0136	0.0120	0.0109	0.0104	0.0142	0.0182	0.0188	0.0178
5988	0.0033	0.0070	0.0084	0.0087	0.0083	0.0088	0.0100	0.0122	0.0128	0.0109	0.0089	0.0094
6923	0.0037	0.0078	0.0091	0.0092	0.0090	0.0084	0.0083	0.0109	0.0127	0.0133	0.0153	0.0132

As seen, maximum of the average story drifts occurs at the 2nd, 6th, and 8th stories of the 4, 8, and 12-story buildings, respectively. These values are matched with the maximum damage indices of the buildings for regression analysis.

2.6. Derivation of the conversion equation

After determining the stories with largest maximum drifts in 4, 8, and 12-story structures, the data obtained for each structure under each one of the 11 earthquake motions is transferred to the (Damage index, Drift ratio) plane, as shown for instance for the 4-story building in Figure 7.

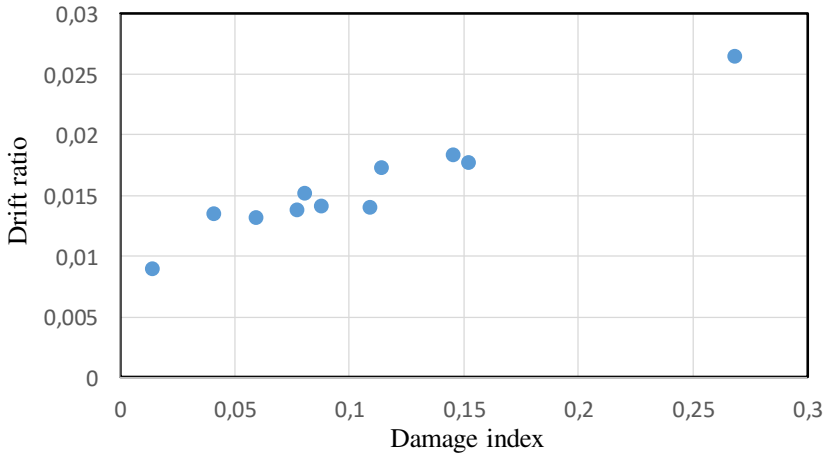

Fig. 7. The maximum damage index vs the maximum drift for the 4-story building under 11 earthquakes.

Figure 7 cannot be used to derive a regression equation for the maximum drift correlated to the damage index because it covers only a small part of the 0-1 range for the damage index. The maximum damage index observed in this figure is about 0.27 that is in the repairable range. It is expected because the studied buildings have been designed based on the current building codes. To cover a wider range, it is decided to utilize the incremental dynamic analysis (IDA), i.e., to calculate the damage index for the same ground motion when scaled up to have progressively larger peak ground accelerations. Performing this way results in much more populated (Damage index, Drift ratio) points as observed in Fig. 8.

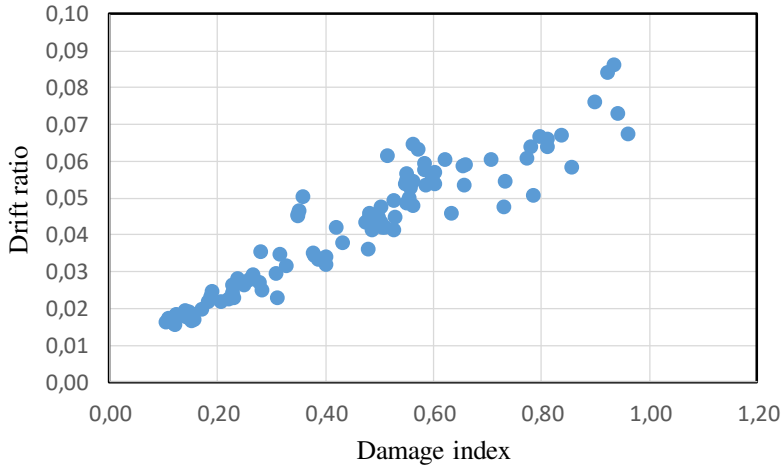

Fig. 8. Maximum damage index vs maximum drift for the 4-story building; IDA analysis with 11 earthquakes.

A curve fitting process is then followed for the data of Fig. 8 for the 4-story building, and similarly for the other ones, using different curves. This results in Fig. 9, where linear, quadratic, cubic, and power regressions are tested.

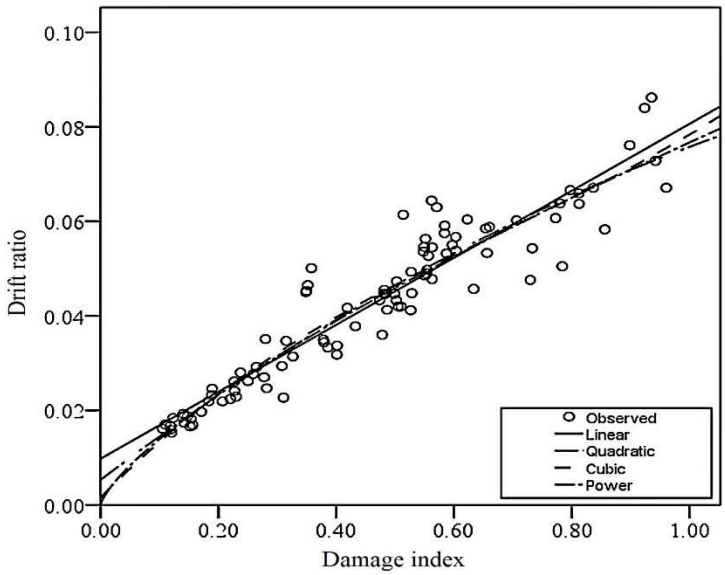

(a)

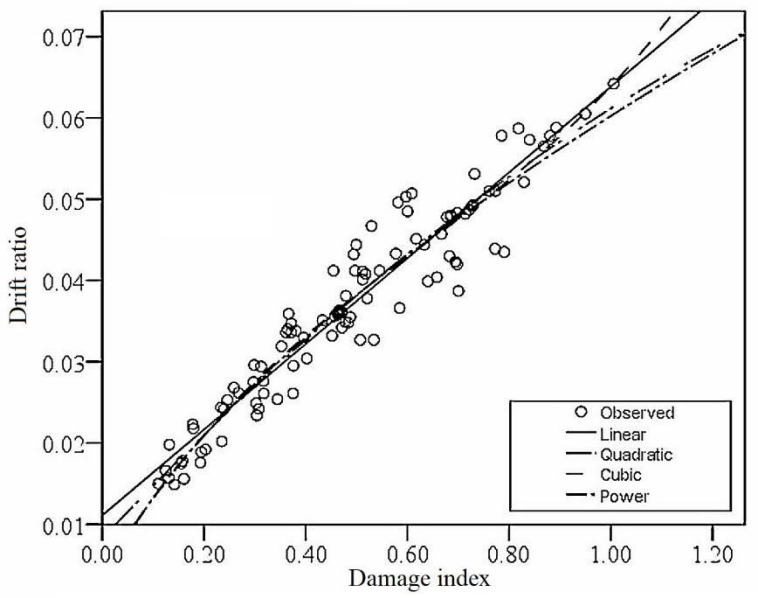

(b)

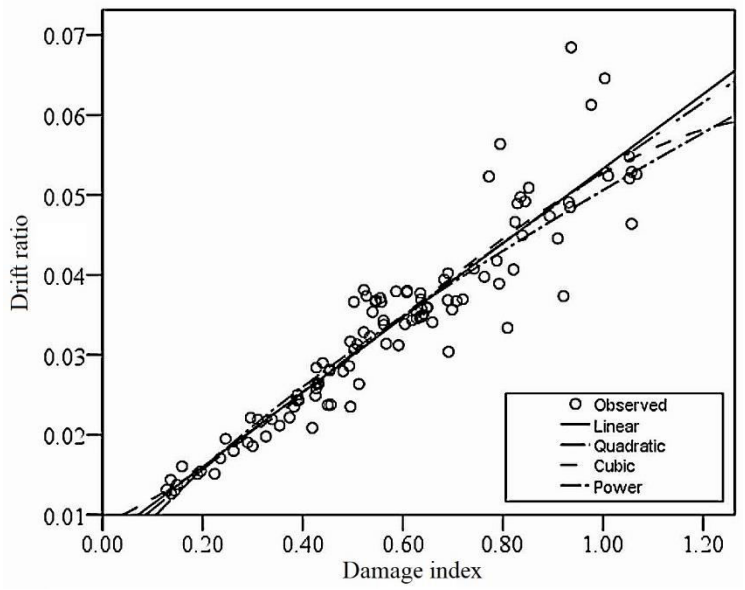

(c)

Fig. 9. Regression analysis for the buildings. (a) 4-story, (b) 8-story, and, (c) 12-story buildings.

Values of the R-square parameter are shown in Table 4 for each building and each regression shape.

Table 4. The R-square factor (R^2).

Building	Regression curve	R^2
4-Story	Linear	0.890
	2nd order	0.896
	3rd order	0.897
	power	0.928
8-Story	Linear	0.912

	2nd order	0.915
	3rd order	0.917
	power	0.93
12-Story	Linear	0.875
	2nd order	0.875
	3rd order	0.876
	power	0.915

As observed, the linear regression is both accurate and simple enough to be picked up from within the regression curves. Then, the following relation emerges as the conversion equation:

$$U = a \cdot DI + b \tag{7}$$

where U is the design story drift, DI is the desired damage index, and a and b are constants. Table 5 shows values of a and b for the studied buildings.

Table 5. Values of the regression parameters, Eq. 7.

No. of stories, n	a	b
4	0.071	0.012
8	0.053	0.011
12	0.047	0.007

Suitably based on Table 5, again linear regression equations between other options, are derived for a and b as functions of n:

$$\begin{aligned} a &= -0.003\, n + 0.081 \\ b &= -0.0006\, n + 0.015 \end{aligned} \tag{8}$$

Equations 7 and 8 are valid for moment frame building at least up to 12 stories.

3. Design of the buildings based on damage

The damage-based seismic design procedure proposed in this study consists of selecting a damage index and then calculating its associated design drift ratio using Eq. (7). The latter quantity is input to the displacement-based design procedure outlined in DBD 12 [15].

As a guide to selecting the desired damage index, Table 7 is presented. In this table, each range of the damage index is described with its corresponding damage extent.

Table 6. The damage intensity for each range of the damage index [22].

Park-Ang DI	Damage intensity	Performance level
0.0-0.2	Minor	Operational
0.2-0.5	Moderate	Life safety
0.5-1	Severe	Near collapse
>1	Collapse	Total collapse

Steps of the procedure are presented for instance for DI=0.4, as follows:

Step 1. DI=0.4 → U = 0.040, 0.033, and 0.026 for 4, 8, and 12 story buildings, respectively, using Eq. 7.

Step 2. Determining the lateral displacement of story *i*, Δ_i , from Eq. (9):

$$\Delta_i = \omega_\theta \Delta_{i,LS} - \theta_{N,i} \cdot x_{CP_i - CM_i} \tag{9}$$

in which ω_θ is the displacement reduction factor due to higher modes effect, $\Delta_{i,Ls}$ is lateral displacement of the center of mass of the *i*-th story at the selected limit state, $\theta_{N,i}$ is the torsion angle of the *i*-th story when its displacement is maximum, and $x_{CP_i - CM_i}$ is distance between the critical point and the mass center of the *i*-th story. ω_θ equals unity for moment frame buildings up to 6 stories and equals 0.85 when number of stories is 16 and larger. It is calculated by linear interpolation in between. $\Delta_{i,Ls}$ is calculated using Eq. (10):

$$\Delta_{i,LS} = \frac{(4H_n - h_i)}{(4H_n - h_1)} \cdot \theta_c h_i \tag{10}$$

where h_i is height of the *i*-th floor from the base level, H_n is the total height of the building from the same level, θ_c is the design drift ratio calculated in step 1, and h_1 is height of the first story.

Step 3. Calculating the equivalent SDF system characteristics, including the target displacement Δ_d, the effective mass m_e, equivalent height h_e, ductility factor μ, and damping ratio ζ , as follows:

$$\Delta_d = \frac{\sum_{i=1}^{n} m_i \Delta_i^2}{\sum_{i=1}^{n} m_i \Delta_i} \tag{11}$$

$$m_e = \frac{\sum_{i=1}^{n} m_i \Delta_i}{\Delta_d} \tag{12}$$

$$h_e = \frac{\sum_{i=1}^{n} m_i \Delta_i h_i}{\sum_{i=1}^{n} m_i \Delta_i} \tag{13}$$

$$\mu = \left(\frac{\Delta_d}{\Delta_y}\right) \geq 1 \tag{14}$$

$$\zeta = 0.05 + 0.577\left(\frac{\mu - 1}{\pi\mu}\right) \tag{15}$$

in which m_i is mass of the *i*-th story, *n* is number of stories, and Δ_y is the effective yield displacement calculated as:

$$\Delta_y = H_e \cdot \theta_y \tag{16}$$

where θ_y is the effective yield drift as:

$$\theta_y = 0.65 \varepsilon_y L_b / h_b \tag{17}$$

in which ε_y is the yield strain of steel, L_b is the average span length, and h_b is the average depth of the beams of the story.

Step 4. Determining the elastic and inelastic design displacement spectra. The elastic design displacement spectrum, S_d , is calculated from the following well known equation:

$$S_d(T) = \frac{T^2}{4\pi^2} S_a(T) \cdot g \tag{18}$$

where T is the natural period, S_a is the design acceleration spectral value, and g is acceleration of gravity. S_d is calculated using Fig. 1. It is shown in Fig. 10.

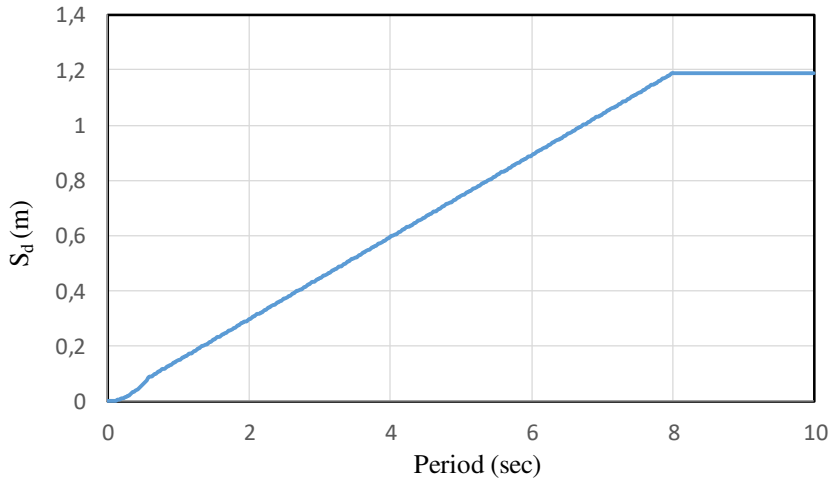

Fig. 10. The design displacement spectrum.

The inelastic design displacement spectrum is determined by multiplying S_d by the factor R_ξ .This factor is a function of the equivalent damping ratio ξ and fault distance as follows:

$$R_\zeta = \left(\frac{0.07}{0.02 + \zeta} \right)^{0.5} \quad : \quad \text{at far distances from fault} \tag{19-a}$$

$$R_\zeta = \left(\frac{0.07}{0.02 + \zeta} \right)^{0.25} \quad : \quad \text{at near distances to fault} \tag{19-b}$$

Step 5. Calculating the effective period and stiffness. The effective period T_e is extracted from the inelastic spectrum at the target displacement Δ_d. Then the effective stiffness k_e is determined as follows:

$$k_e = \frac{4\pi^2 m_e}{T_e^2} \tag{20}$$

Step 6. Determining the base shear, V_{Base} , as:

$$V_{\text{Base}} = k_e \Delta_d + V_{P-\Delta} < 2.5 R_\zeta \cdot PGA \cdot m_e + V_{P-\Delta} \tag{21}$$

where $V_{P\text{-}\Delta}$ is the base shear due to the P-Δ effect. It is calculated as follows:

$$V_{P-\Delta} = C \cdot \frac{P\Delta_d}{H_e} = C \cdot \frac{m_e g \Delta_d}{H_e} \qquad (\Delta_y > \Delta_d) \tag{22-a}$$

$$V_{P-\Delta} = C \cdot \frac{P\Delta_y}{H_e} = C \cdot \frac{m_e g \Delta_y}{H_e} \qquad (\Delta_y < \Delta_d) \tag{22-b}$$

Step 7. Calculating the design lateral forces, F_i , as:

$$F_i = 0.9\, V_{\text{Base}} \left(m_i \Delta_i\right) \Big/ \left(\sum_{j=1}^{n} m_j \Delta_j\right) \quad : \text{For all floors except the roof floor} \tag{23-a}$$

$$F_n = 0.1\, V_{\text{Base}} + 0.9\, V_{\text{Base}} \left(m_n \Delta_n\right) \Big/ \left(\sum_{j=1}^{n} m_j \Delta_j\right) \quad : \text{For the roof floor} \tag{23-b}$$

Then, the structural system is designed for the member forces due to application of the above lateral forces. Use of the above procedure results in the following table that lists values of the mentioned parameters for the buildings of this study.

Table 7. Values of the design parameters of the buildings.

Parameter	No. of stories		
	4	8	12
ω_θ	1.000	0.970	0.910
$\Delta_d\,(m)$	0.299	0.432	0.524
$m_e\,(ton)$	580.374	1118.917	1477.553
$H_e\,(m)$	9.251	17.532	25.839
$h_b\,(m)$	0.285	0.299	0.348
$\theta_y\,(rad)$	0.014	0.013	0.011
$\Delta_y\,(m)$	0.127	0.229	0.289
μ	2.361	1.888	1.811
ζ	0.156	0.136	0.132
R_ζ	0.631	0.669	0.678
$T_e\,(\text{sec})$	3.060	4.950	5.620
$k_e\,(kN/m)$	2446.947	1802.799	1846.844
$k_e \cdot \Delta_d\,(kN)$	731.209	777.988	967.939
$V_{P-\Delta}(kN)$	77.911	143.093	162.383
$V_{Base}\,(kN)$	809.119	921.081	1130.322

Design of the buildings based on the above procedure that began with setting DI at 0.4, results in the fundamental periods of the new buildings to be 1.32, 2.35, and 2.76 sec for the 4, 8, and 12-story buildings, respectively. They can be compared with the forced-based design period that, as mentioned in Sec. 2.2, are 1.02, 1.82, and 2.24 sec. Sections of the beams appear to be IPE240 to IPE330, IPE240 to IPE360, and IPE240 to IPE450, for the same order of buildings. The column box sections are 180×20 to 300×20, 180×20 to 340×20, and 220×20 to 440×30, respectively.

4. Nonlinear dynamic analysis of the damage-based designed buildings

The buildings designed in Sec. 3 according to the damage-based procedure, are analyzed nonlinearly under the ground motions introduced in Sec. 2.4. The maximum damage index in each story under each earthquake is reported in Table 8.

Table 8. Maximum damage index in each case for the damage-based designed buildings. (a) 4-story, (b) 8-story, and (c) 12-story building.

(a)

NGA No.	Story 1	Story 2	Story 3	Story 4
	Story Damage Index			
20	0.300	0.124	0.075	0.028
68	0.073	0.060	0.028	0.012
169	0.277	0.198	0.129	0.046
778	0.095	0.097	0.061	0.032
826	0.109	0.111	0.078	0.018
900	0.443	0.271	0.192	0.070
987	0.036	0.039	0.007	0.005
1107	0.111	0.052	0.032	0.042
4853	0.209	0.161	0.087	0.027
5814	0.254	0.222	0.231	0.139
6923	0.043	0.064	0.075	0.062
Max DI	0.443	0.271	0.231	0.139
Ave of Max DI	0.177	0.127	0.090	0.044

(b)

NGA No.	Story 1	Story 2	Story 3	Story 4	Story 5	Story 6	Story 7	Story 8
	Story Damage Index							
20	0.014	0.054	0.155	0.198	0.169	0.083	0.027	0.024
68	0.032	0.028	0.030	0.014	0.010	0.019	0.014	0.024
169	0.009	0.125	0.268	0.389	0.394	0.258	0.131	0.051
778	0.330	0.314	0.387	0.358	0.307	0.234	0.184	0.100
900	0.014	0.037	0.064	0.072	0.150	0.163	0.096	0.029
987	0.007	0.004	0.025	0.033	0.037	0.071	0.043	0.007
1110	0.030	0.113	0.160	0.115	0.071	0.159	0.135	0.046
4849	0.014	0.063	0.149	0.172	0.155	0.144	0.077	0.019
5814	0.045	0.122	0.159	0.133	0.092	0.114	0.166	0.102
5988	0.007	0.054	0.078	0.055	0.025	0.037	0.024	0.033
6923	0.014	0.059	0.082	0.067	0.049	0.042	0.018	0.024
Max DI	0.330	0.314	0.387	0.389	0.394	0.258	0.184	0.102
Ave of Max DI	0.047	0.088	0.142	0.146	0.133	0.120	0.083	0.042

(c)												
NGA no.	Story1	Story 2	Story 3	Story 4	Story 5	Story 6	Story 7	Story 8	Story 9	Story 10	Story 11	Story 12
	Story Damage Index											
20	0.014	0.010	0.040	0.057	0.112	0.183	0.205	0.168	0.116	0.056	0.026	0.045
68	0.036	0.022	0.068	0.084	0.100	0.115	0.098	0.059	0.030	0.027	0.020	0.074
169	0.014	0.070	0.122	0.170	0.292	0.238	0.243	0.254	0.251	0.163	0.065	0.057
777	0.027	0.160	0.252	0.250	0.213	0.220	0.241	0.223	0.234	0.201	0.120	0.063
900	0.019	0.056	0.104	0.102	0.072	0.039	0.028	0.070	0.096	0.094	0.073	0.073
987	0.001	0.006	0.009	0.009	0.012	0.005	0.001	0.000	0.001	0.016	0.012	0.038
1110	0.034	0.028	0.041	0.049	0.049	0.031	0.025	0.043	0.083	0.080	0.055	0.064
4849	0.030	0.037	0.039	0.043	0.045	0.061	0.098	0.104	0.079	0.063	0.043	0.043
5814	0.022	0.172	0.341	0.406	0.402	0.365	0.275	0.196	0.137	0.118	0.099	0.079
5988	0.029	0.039	0.113	0.139	0.134	0.121	0.088	0.046	0.024	0.032	0.028	0.066
6923	0.022	0.029	0.069	0.088	0.076	0.066	0.062	0.056	0.037	0.026	0.021	0.054
Max DI	0.036	0.172	0.341	0.406	0.402	0.365	0.275	0.254	0.251	0.201	0.120	0.079
Ave of Max DI	0.022	0.057	0.109	0.127	0.137	0.131	0.124	0.111	0.099	0.080	0.051	0.059

As observed, in the most critical cases, the damage index is just close to the DI taken for design of the mentioned building. Then it can be said that the procedure of matching the desired DI with a design drift and the displacement-based design afterwards, has been successful in limiting the maximum DI under the spectrum-compatible ground motions to the desired value. As seen in Table 8, for medium and repairable damage, DI should be contained within 0.2-0.4. To investigate further, the above procedure is repeated this time for DI=0.2. In this case, the design drift ratio becomes 0.021, 0.018 and 0.014 for 4, 8, and 12-story buildings, respectively. Then heavier sections are designed for the members. The design sections for the beams are IPE270 to IPE360, IPE300 to IPE400, and IPE300 to IPE500 for the mentioned buildings. The column box sections are 180×20 to 300×20, 180×20 to 340×20, and 220×20 to 440×20 for the same buildings. The fundamental periods are 0.93, 1.64, and 2.02 sec, respectively. The maximum damage index in each case is shown in Table 9.

Table 9. Maximum damage index for DI=0.2 for the damage-based designed buildings.

(a)				
NGA No.	Story 1	Story 2	Story 3	Story 4
	Story Damage Index			
20	0.154	0.123	0.083	0.011
68	0.004	0.018	0.023	0.005
169	0.143	0.081	0.062	0.010
778	0.103	0.076	0.072	0.014
826	0.020	0.037	0.037	0.003
900	0.087	0.087	0.061	0.007
987	0.043	0.080	0.041	0.000
1107	0.067	0.053	0.052	0.016
4853	0.156	0.110	0.074	0.007

5814	0.220	0.178	0.151	0.118
6923	0.032	0.033	0.061	0.045
Max DI	0.220	0.178	0.151	0.118
Ave of Max DI	0.093	0.080	0.065	0.022

(b)

NGA No.	Story 1	Story 2	Story 3	Story 4	Story 5	Story 6	Story 7	Story 8
	Story Damage Index							
20	0.1585	0.1909	0.2127	0.2053	0.1536	0.0420	0.0173	0.0002
68	0.0001	0.0002	0.0002	0.0003	0.0003	0.0003	0.0002	0.0001
169	0.0748	0.0929	0.1065	0.0994	0.0857	0.0873	0.0679	0.0108
778	0.1424	0.0985	0.1006	0.1317	0.1330	0.0821	0.0394	0.0004
900	0.0010	0.0347	0.0504	0.1361	0.1981	0.1584	0.0830	0.0056
987	0.0006	0.0257	0.0480	0.0344	0.0149	0.0310	0.0144	0.0001
1110	0.0067	0.0570	0.0788	0.0589	0.0456	0.0477	0.0332	0.0004
4849	0.1270	0.2046	0.2272	0.2143	0.2023	0.1346	0.0783	0.0011
5814	0.0345	0.0876	0.1056	0.0928	0.1251	0.1595	0.1494	0.0826
5988	0.0058	0.0557	0.0973	0.1531	0.1674	0.1169	0.0484	0.0003
6923	0.0823	0.1127	0.1196	0.0971	0.0805	0.0492	0.0277	0.0008
Max DI	0.1585	0.2046	0.2272	0.2143	0.2023	0.1595	0.1494	0.0826
Ave of Max DI	0.0576	0.0873	0.1043	0.1112	0.1097	0.0826	0.0508	0.0093

(c)

NGA no.	Story1	Story 2	Story 3	Story 4	Story 5	Story 6	Story 7	Story 8	Story 9	Story 10	Story 11	Story 12
	Story Damage Index											
20	0.001	0.038	0.102	0.174	0.212	0.224	0.187	0.124	0.063	0.043	0.021	0.027
68	0.000	0.004	0.009	0.006	0.003	0.002	0.001	0.024	0.041	0.036	0.034	0.026
169	0.006	0.082	0.122	0.136	0.114	0.117	0.114	0.166	0.123	0.065	0.037	0.029
777	0.152	0.168	0.197	0.205	0.209	0.226	0.211	0.190	0.178	0146	0.079	0.033
900	0.001	0.027	0.052	0.067	0.078	0.114	0.158	0.186	0.160	0.087	0.056	0.033
987	0.001	0.024	0.039	0.031	0.013	0.004	0.007	0.050	0.078	0.067	0.031	0.015
1110	0.004	0.060	0.091	0.092	0.083	0.087	0.086	0.098	0.156	0.170	0.101	0.045
4849	0.003	0.065	0.121	0.151	0.161	0.115	0.174	0.167	0.133	0.078	0.035	0.022
5814	0.013	0.140	0.186	0.190	0.158	0.117	0.095	0.075	0.115	0.169	0.138	0.091
5988	0.002	0.030	0.046	0.045	0.042	0.047	0.059	0.062	0.033	0.013	0.008	0.037
6923	0.003	0.044	0.052	0.036	0.016	0.015	0.045	0.055	0.065	0.039	0.015	0.021
Max DI	0.152	0.168	0.197	0.205	0.212	0.226	0.211	0.190	0.178	0.170	0.138	0.091
Ave of Max DI	0.017	0.062	0.093	0.103	0.099	0.097	0.103	0.109	0.104	0.083	0.050	0.035

Again, as observed, the proposed damage-based procedure has been successful in limiting the resulting maximum damage index in the most critical case for each building to the presumed value.

For comparison, in the following three tables, the fundamental periods, base shear, and total member weights of the damage-based designed buildings are compared with their force-based counterparts.

Table 10. Comparison of the fundamental periods.

No. of stories	Fundamental period (Sec)			Ratio of	Ratio of
	DI=0.2	DI=0.4	Force-based	column 2 to 4	column 3 to 4
4	0.93	1.32	1.02	0.91	1.29
8	1.64	2.35	1.82	0.90	1.29
12	2.02	2.76	2.24	0.90	1.23

Table 11. Comparison of base shears.

No. of stories	Base shear (kN)			Ratio of	Ratio of
	DI=0.2	DI=0.4	Force-based	column 2 to 4	column 3 to 4
4	968.38	809.12	862.67	1.12	0.94
8	1048.53	921.08	965.63	1.09	0.95
12	1293.07	1130.32	1180.62	1.10	0.96

Table 12. Comparison of total structure weight.

No. of stories	Total structure weight (tonf)			Ratio of	Ratio of
	DI=0.2	DI=0.4	Force-based	column 2 to 4	column 3 to 4
4	42.60	38.30	40.79	1.04	0.94
8	98.25	86.69	92.61	1.06	0.94
12	201.88	181.54	190.03	1.06	0.96

As observed, by halving DI, the structure's weight increases only up to 10% compared with the force-based design that may justify such a strictness if architectural and mechanical limitations allow. Moreover, the base shear increases up to 12% and the period reduces up to 10% for DI=0.2 compared with the force-based quantities. By observation, it seems that the force-based procedure is consistent approximately with DI=0.3. Then, the proposed design procedure is flexible enough to make and compare different designs regarding the acceptable damage for the final decision.

5. Conclusions

A procedure for practical damage-based design of moment-frame structures under seismic loads was presented in this paper. In this method, a design drift ratio was devised based on the desired damage index. For this purpose, the Park-Ang damage index was calculated for 4, 8, and 12-story special steel moment frame buildings designed based on the conventional force-based procedure. Eleven pairs of ground motions were selected and scaled to a design spectrum for nonlinear dynamic analysis. The maximum values of drift ratio and its associated damage index were extracted from the analysis under each earthquake in each story. Use of the pairs of maximum (drift ratio, damage index) resulted in a linear regression equation converting one of the mentioned parameters to the other for each building. By

selecting two different values as the desired damage indices, the design drifts were calculated for both cases and the buildings were designed in the context of displacement-based design. After performing nonlinear dynamic analysis on the designed buildings, maximum damage indices were calculated and reported for each story under each earthquake. Finally, it was concluded that:

1. The proposed procedure begins from selecting a damage index. Then it simply proceeds to calculate the design drift from the developed regression equation and then to other design parameters. It makes a practical step by step trend for seismic design.

2. Results of the damage-based design are in good correlation with the forced-based design. It can be assumed that the force-based design is for a damage index of about 0.3 inherently.

3. For the 11 pairs of spectrum compatible ground motions, the damage-based design resulted in maximum story damage indices that in the worst case just meet the design damage index. The average values are clearly smaller and they are on the order of 60-70% of the maximum values. Then the design is safe enough.

4. The developed equation for converting the design damage index to the design drift ratio appears to be simply a linear relation with good correlation. Use of this simple equation resulted in acceptable story damage indices in the most critical cases studied.

6. Declarations

6.1. Funding

Not applicable.

6.2. Conflicts of interest/Competing interests

Not applicable.

6.3. Availability of data and material

Data underlying the results is available at reasonable request from the first author.

6.4. Code availability

The computational code for the research is available at reasonable request from the first author.

6.5. Authors' contributions

All authors contributed to the study conception and design. Data collection and analysis were performed by Ali Hosseini-Rad. The first draft of the manuscript was written by Farhad Behnamfar and all authors commented on previous versions of the manuscript. All authors read and approved the final manuscript.

6.6. Ethics approval

Not applicable.

6.7. Consent to participate

All authors consented to participate in this research.

6.7. Consent for publication

All authors consented to publish the results of this research.

7. References

[1] T. J. Sullivan, M. J. N. Priestley and G.M. Calvi. DBD12: A Model Code for the Displacement-Based Seismic Design of Structures, *Iuss Press*, Pavia, 2012.

[2] G. H. Powell and R. Allahabadi, Seismic damage prediction by deterministic methods: concepts and procedures, *Earthquake Engineering & Structural Dynamics,* Vol. 16, No. 5, pp. 719-734, 1988.

[3] H. Krawinkler and M. Zohrei, Cumulative damage in steel structures subjected to earthquake ground motions, *Computers & Structures,* Vol. 16, No. 1-4, pp. 531-541, 1983.

[4] Y. Bozorgnia and V. V. Bertero, Evaluation of damage potential of recorded earthquake ground motion, *Seismological Research Letters*, Vol. 72, pp. 233-233, 2001.

[5] Y. Park, A. H. Ang, and Y. Wen, Damage-limiting aseismic design of buildings, *Earthquake spectra,* Vol. 3, No. 1, pp. 1-26, 1987.

[6] S. K. Kunnath, A. M. Reinhorn, and R. Lobo, IDARC Version 3.0: A program for the inelastic damage analysis of reinforced concrete structures. National Center for Earthquake Engineering Research Buffalo, NY, 1992.

[7] P. Panyakapo, Seismic capacity diagram for damage based design, in *Proceedings of 14th World Conference on Earthquake Engineering. Beijing, China*, 2008.

[8] H. Jiang, B. Fu, and L. Chen, Damage-control seismic design of moment-resisting RC frame buildings, *Journal of Asian Architecture and Building Engineering,* Vol. 12, No. 1, pp. 49-56, 2013.

[9] G. S. Kamaris, G. D. Hatzigeorgiou, and D. E. Beskos, Direct damage controlled seismic design of plane steel degrading frames, *Bulletin of Earthquake Engineering,* Vol. 13, No. 2, pp. 587-612, 2014.

[10] G. S. Kamaris, G. D. Hatzigeorgiou, and D. E. Beskos, A new damage index for plane steel frames exhibiting strength and stiffness degradation under seismic motion, *Engineering Structures,* Vol. 46, pp. 727-736, 2013.

[11] K. Ke and M. C. Yam, A performance-based damage-control design procedure of hybrid steel MRFs with EDBs, *Journal of Constructional Steel Research,* Vol. 143, pp. 46-61, 2018.

[12] H. Estekanchi and K. Arjmandi, Comparison of damage indexes in nonlinear time history analysis of steel moment frames, *Asian Journal of Civil Engineering (Building and Housing)*, Vol. 8, No. 6, pp. 629-646, 2007.

[13] M. S. Kazemi, F. Behnamfar, Active control of structures based on an arbitrary damage index distribution, *AUT Journal of Civil Engineering*, Vol. 4, No. 3, pp. 385-396, 2020.

[14] ASCE7-16. Minimum design loads and associated criteria for buildings and other structures. American Society of Civil Engineers (ASCE), pp. 1-889, 2016.

[15] AISC 360-10. Specification for structural steel buildings. *American Institute of Steel Construction (AISC), Chicago*, 2010.

[16] OpenSees. Open system for earthquake engineering simulation. Pacific Earthquake Engineering Center. University of California, Berkeley, CA.

[17] ASCE/SEI 41-17. Seismic Evaluation and Retrofit of Existing Buildings. A*merican Society of Civil Engineers*, 2017.

[18] M. Rahnama and H. Krawinkler, Effects of soft soil and hysteresis model on seismic demands. John A. Blume Earthquake Engineering Center, Stanford University, Rep. Vol. 108, No. TB, 1993.

[19] D. G. Lignos and H. Krawinkler, Deterioration modeling of steel components in support of collapse prediction of steel moment frames under earthquake loading, *Journal of Structural Engineering,* Vol. 137, No. 11, pp. 1291-1302, 2011.

[20] D. Farahani, F. Behnamfar, H. Sayyadpour, and M. Ghandil, Seismic impact between adjacent torsionally coupled buildings, *Soil Dynamics and Earthquake Engineering,* Vol. 117, pp. 81-95, 2019.
[21] PEER strong ground motion database [Online] Available: https://ngawest2.berkeley.edu.
[22] M. Komeili, A. S. Milani, and S. Tesfamariam, Performance-based earthquake engineering design of reinforced concrete structures using black-box optimisation, *International Journal of Materials and Structural Integrity,* Vol. 6, No. 1, pp. 1-25, 2012.